Scientific Research Publishing

Advances in Biological Chemistry, 2025, 15(1), 1-17
https://www.scirp.org/journal/abc
ISSN Online: 2162-2191
ISSN Print: 2162-2183

Synthesis, Characterization, and Cell Viability Evaluation of Coordination Compounds with Rhodium(III) Ion and Nitrogen-Containing Heterocyclic Ligands

Vanessa Souza da Silva[1*], Rans Miler Pereira Dantas[1], Maria José Santos Mesquita[1], Bruna Alves Rodrigues[1], Sara Cristina Bernardes Correia[1], Dayanne Oliveira da Silva Mendes[1], Aron Carlos de Melo Cotrim[2], Joyce Laura da Silva Gonçalves[1], Wagner Batista dos Santos[1*]

[1]Institute of Exact and Earth Sciences, Federal University of Mato Grosso, Barra do Garças, MT, Brazil
[2]Institute of Biological and Health Sciences, Federal University of Mato Grosso, Barra do Garças, MT, Brazil
Email: *vanessa.s.silva@edu.mt.gov.br, *wbsantos@ufmt.br

How to cite this paper: da Silva, V.S., Dantas, R.M.P., Mesquita, M.J.S., Rodrigues, B.A., Correia, S.C.B., da Silva Mendes, D.O., de Melo Cotrim, A.C., da Silva Gonçalves, J.L. and dos Santos, W.B. (2025) Synthesis, Characterization, and Cell Viability Evaluation of Coordination Compounds with Rhodium(III) Ion and Nitrogen-Containing Heterocyclic Ligands. *Advances in Biological Chemistry*, **15**, 1-17.
https://doi.org/10.4236/abc.2025.151001

Received: November 5, 2024
Accepted: January 17, 2025
Published: January 20, 2025

Abstract

In the search for new drugs with more efficient active ingredients, various transition metals are being explored as potential metallopharmaceuticals. These compounds, which combine drugs with metals, have shown promise as chemotherapeutic agents, akin to the accidental discovery of cisplatin and its organic derivatives in the late 20th century. This discovery transformed the sciences, particularly in the fields of organic and inorganic chemistry, by offering new insights into the compositions and molecular geometries of inorganic complexes through coordination chemistry, while also intersecting with other scientific domains such as pharmacology and medicine. To contribute to the development of new chemotherapeutic compounds through simple and reproducible synthetic processes, this study utilized rhodium(III) chloride hydrate ($RhCl_3.nH_2O$) to synthesize a series of compounds with the following organic *N*-heterocyclic ligands: 4,4'-dimethyl-2,2'-bipyridine, isonicotinamide, and *N*-(3-pyridyl)-isonicotinamide (3-pina). Two analytical techniques were employed to characterize the resulting materials: spectroscopic analysis in the infrared region, which suggested interactions and substitutions at the metal center by the organic compounds, and thermoanalytical analyses, which led to the proposal of minimum formulas for the compounds as follows: C1 $[RhCl_2(4,4'\text{-Met-}2,2'\text{-bipy})_2]Cl{\cdot}5/2H_2O$ and C2 $[Rh(4,4'\text{-Met-}2,2'\text{-bipy})2(Iso)_2]Cl_3{\cdot}1/2H_2O$. However, the complexation of the third compound could not be confirmed due to the physicochemical characteristics of the resulting complex being very similar to those of the starting material, thereby validating the

effectiveness of these techniques in differentiating and characterizing the synthesized salts. Due to their solubility in water and/or alcohol and thermal stability, the complexes were tested in biological media to assess cell viability in peripheral blood mononuclear cells. The solutions of these salts demonstrated favorable cell viability under the tested conditions, according to statistical analysis, obtaining average viability in the range of $95 \leq x \leq 100$, with standard deviations between $3.29 \leq x \leq 4.44$ for living cells.

Keywords

Rhodium, N-Heterocyclics, 4,4-Met-2,2-Bipyridine, Isonicotinamide, 3-Pina, Metallopharmaceuticals, Thermoanalytics

1. Introduction

Estimates from the World Health Organization (WHO) suggest that by 2050 [1], [2] there will be a significant increase in mortality worldwide due to the ineffectiveness of existing medications in combating various harmful microbial agents. These agents are considered exacerbating factors in clinical complications in patients with comorbidities, leading to an increase in death rates [3] [4]. According to the International Agency for Research on Cancer, there were approximately 20 million new cases of cancer in 2022, resulting in the deaths of 9.7 million people. However, research indicates that around 40% of these deaths could have been prevented [2] [5]. It is estimated that one in nine men and one in twelve women die due to clinical complications from viral, bacterial, or parasitic infections [6]. In 2017, the WHO alerted the scientific community by compiling a list of twelve bacterial strains posing a global threat to human health because of antimicrobial resistance [1].

In 2024, the Pan American Health Organization highlighted this issue, especially in underdeveloped countries, emphasizing the necessity for financial investment in scientific research to address this issue and the need to regulate public intervention and monitoring policies to enhance the effectiveness of the various existing clinical treatments [2] [7]. Since 1969, new inorganic compounds, such as cisplatin, have been synthesized and characterized in the fields of organometallic chemistry, materials chemistry, nanomaterials, inorganic chemistry, and bioinorganic chemistry [8]-[10]. Consequently, ongoing research seeks to find new materials to improve quality of life and survival by decelerating the global mortality rate through the development of more effective medications [11].

Platinum complexes have significantly contributed to the growth of scientific production in therapeutic chemistry worldwide. Nonetheless, their toxicity limits their market presence in the production of active ingredients containing this noble metal [12]-[15]. New research directions include drugs based on metals such as Cu(II), Ni(II), and Co(II), which were active against intracellular amastigotes of *Leishmania braziliensis* and showed *in vivo* efficacy against the Leishmania-

related trypanosomatids, *Trypanosoma cruzi*, by reducing parasitemia by 83% [15], demonstrating the potential for producing complex and bioactive inorganic substances with these transition metals. Additionally, new transition metals, including ruthenium complexes like cis-[$RuCl_2(NH_3)$] Cl, have exhibited antitumor activity against tumor cell lines such as Jurkat SK-BR-3 and induced lethal effects in human chronic myeloid leukemia K562 cells [16]. Other compounds undergoing clinical stage studies, including Ru(III) (Nami-A, KP1019, and RAPTA-C) and platinum complexes, demonstrated antimetastatic activity [17] [18], though they failed the final clinical stage [19].

Gold(I) and (III) complexes synthesized with heterocyclic compounds containing five-membered rings have also become significant due to their versatile biological properties [20] [21]. Studies on organic N-heterocyclic compounds featuring the 1,3,4-oxadiazole portion have shown antimicrobial, anticancer, and antiviral activities [22]. Likewise, complexes of noble metals with N-heterocyclic ligands have been contributing as future drugs for anti-neoplastic, antiparasitic, antiviral, and antimicrobial uses [23]. A study such as the use of nitrenium cation to the metal centers Rh I, Rh III, corroborates the discovery of new complexes with N-Heterocyclic ligands [24]. Therefore, the choice of N-heterocyclic compounds is justified, since these ligands can coordinate with Platinum Group Metal ions (PGM) [25]. Nevertheless, advances in the studies for obtaining new metallopharmaceuticals encounter specific difficulties, among them the challenge of understanding biomolecular interactions [21].

Thus, the importance of new inorganic studies with this promising metal is to provide new pathways for the synthesis and characterization of complexes with N-heterocyclic ligands to rhodium(III) ions. Therefore, the present work aims at new syntheses and characterizations of possible new rhodium metallopharmaceuticals that allow for the structural stability of coordination complexes and thus their high selectivity as a potential active principle, thereby minimizing the commonly reported adverse effects to enable efficiency in treating various pathologies as well as expanding the possibilities of combating various resistant microbial agents.

2. Syntheses

2.1. Synthesis of the N-(3-Pyridyl)-Isonicotinamide Ligand

The synthesis of the N-(3-pyridyl)-isonicotinamide (3-pina) ligand was carried out following the procedure described by Gardner and colleagues [26] and later modified by Encarnação Amorim [25]. Reagents including 3.0090 g of 3-aminopyridine and 5.6500 g of Isonicotinoyl chloride hydrochloride were prepared. These were dissolved in 60.0 mL of pyridine in a 250.0 mL volumetric flask. The mixture was then sealed and stirred magnetically for 4 days. After this period, a biphasic separation occurred, resulting in the formation of a white precipitate. This precipitate was vacuum filtered through filter paper, transferred to a 250.0 mL beaker, and dissolved in 50.0 mL of distilled water. The mixture was then subjected to ultrasonic treatment.

Shortly thereafter, a white solid precipitated and the pH was adjusted to approximately 7 using a spatula tip amount of $NaHCO_3$. Following another filtration step with distilled water, 5.4310 g of a fine, shiny white powder was obtained and dried in a desiccator for 4 days. Once removed and reweighed, its mass was 2.5720 g. The sample underwent Fourier-transform infrared spectroscopy (FTIR), showing characteristic peaks corresponding to those expected. However, further drying in an oven at 90˚C - 100˚C for 24 hours was necessary to remove any residual moisture. Post-oven treatment, 1.2150 g of an opaque white solid was obtained and analyzed again using FTIR.

2.2. Purification and Recrystallization of the N-(3-Pyridyl)-Isonicotinamide Ligand

The purification process was carried out as described in the literature by Encarnação Amorim [27] with some modifications to enhance yield. A total of 0.499 g of the white, amorphous powder was dissolved in hot distilled water (40.0 mL at 70˚C) and stirred on a hot plate for 30 minutes. After reducing the volume to 30.0 mL, the solution was filtered to remove impurities and then cooled in an ice bath to precipitate a translucent crystalline solid resembling small needles. This solid was filtered, dried in a desiccator for 48 hours, weighed, and stored.

2.3. Syntheses of the Starting Compound $[RhCl_2(4,4\text{-Met-}2,2\text{-bipy})_2]Cl{\cdot}nH_2O$

This synthesis was prepared from adaptations of the synthesis reported by Gerisch *et al.* [28]. A solution of 0.3000 g (1.22 mmol) of 4,4'-dimethyl-2,2'-bipyridine in 20.0 mL of ethanol was refluxed, and 0.1500 g (0.56 mmol) of rhodium chloride was added. The mixture was kept under reflux for 4 hours, yielding a light-yellow precipitate. The solvent was then evaporated under reduced pressure until one-third of its original volume remained. The solution was cooled in a refrigerator for 24 hours, and the precipitated solid was collected by filtration, washed with ethanol and ether, and dried under vacuum to yield a light-yellow product.

2.4. Syntheses of the Compound $[Rh(4,4\text{-Met-}2,2\text{-bipy})_2(Iso)_2]Cl{\cdot}nH_2O$

In this assay, 70.0 mg (0.12 mmol) of the initial compound $[RhCl_2(4,4'\text{-Met-}2,2'\text{-Bipy})_2]Cl{\cdot}nH_2O$ was dissolved in 2.0 mL of distilled water in a 50 mL round-bottom flask and treated in an ultrasonic bath with the addition of 5 drops of ethyl alcohol to enhance solubility. Next, 44 mg (0.36 mmol) of Isonicotinamide was added. The reaction mixture was semi-sealed and stirred magnetically for 2 hours, turning yellow. After cooling for 24 hours, a solid precipitated but was found to be soluble at room temperature. The solution was filtered and washed with ether, yielding a yellow solid.

2.5. Purification of the Isonicotinamide Ligand

The purification process followed was described in the literature by Santos [29].

In a beaker, 5 g of Isonicotinamide was dissolved in 15.0 mL of distilled water on a hot plate. Subsequently, 0.5 g of activated charcoal was added, and the mixture was hot filtered. The filtrate was passed through filter paper and/or absorbent cotton in a separating funnel. Upon cooling in an ice bath, a white solid in the form of fine needles precipitated, was filtered again, washed with ether, and stored.

2.6. Syntheses of the Starting Compound with the Ligand N-(3-Pyridyl)-Isonicotinamide

20.0 mg (0.035 mmol) of the starting compound was dissolved in 10 mL of distilled water with 3 drops of ethyl alcohol in a 50.0 mL round-bottom flask to improve the solubility of the ligand. Following the addition of 7.7 mg (0.038 mmol) of the purified reagent 3-pina (1:1), the system was sealed and magnetically stirred at room temperature for 2 hours. The solution was then cooled in an ice bath, but no precipitate formed due to the solubility of the solid in the medium. Consequently, the solvent was evaporated, and after 24 hours, a yellow solid was obtained. This solid was vacuum filtered, washed with ether, and left in a desiccator for 24 hours.

3. Cell Viability Analysis

The biological tests were conducted to gather data on the cell viability of peripheral blood mononuclear cells. These tests followed the methods described in the literature, with some adaptations [30]-[32]. To prepare the 1 mM solutions, 0.0207 g of the compound $RhCl_2(4,4\text{-Met-}2,2\text{-Bibipy})_2]Cl{\cdot}5/2H_2O$ was added to a 25.0 mL volumetric flask, and the volume was adjusted with distilled water. For the modified compound $[Rh(4,4\text{-Met-}2,2\text{-Bibipy})_2(Iso)_2]Cl_3{\cdot}1/2H_2O$, 0.0104 g was added to a 10.0 mL volumetric flask, and the volume was adjusted with distilled water to achieve a concentration of approximately 1 mmol/L.

4. Methodology

The procedure for obtaining peripheral blood mononuclear cells and assessing cell viability involved collecting an average of 5.0 mL of peripheral blood in EDTA-coated tubes from each donor to isolate mononuclear cells. These mononuclear cell populations were then separated using a Ficoll-Paque density gradient (Pharmacia-Uppsala, Sweden) for 40 minutes at 1600 rpm at room temperature. After separation, the layer rich in mononuclear cells was carefully removed by siphoning, and two washes were undergone in phosphate-buffered saline (PBS). The cells were subsequently counted using a Neubauer chamber, and their concentration was adjusted to 2.0×10^6 cells/mL for use in viability assays. The viability of the blood mononuclear cells was determined using fluorescence microscopy and Acridine Orange staining [33] [34].

For viability assessment, 500.0 µL of the mononuclear cell suspension was mixed with 50.0 µL of the test compounds at various concentrations and incubated for 30 minutes in a thermal bath set at 37˚C. Following incubation, the

mixtures were centrifuged for 10 minutes at 1600 rpm, and the cell pellet was then stained with 200.0 μL of acridine orange for 1 minute before being resuspended in PBS. The suspensions were centrifuged and washed twice more with PBS, after which slides were prepared and examined under a fluorescence microscope (E200, Nikon Corporation, Japan). Viability analyses were reported as percentages, based on the observation of 100 cells and classifying them as either alive (green) or dead (orange) according to their differential staining.

4.1. Statistical Analyses

The analysis of variance test followed by Tukey's test was used for statistical analysis in the Bioestat 5.0 software, adopting a significance level of $p < 0.05$.

4.2. Characterization and Methodology

The experimental procedures were conducted at the Laboratory for the Study of Materials (LEMat). Spectroscopic analysis in the infrared region and thermoanalytical analyses (TG/DTG and DSC) were performed at the Multiuser Research Center. Infrared spectroscopy was conducted using a FTIR, specifically the Perkin Elmer Spectrometer 100, featuring a resolution of 4 cm^{-1} in the range of 4000 - 500 cm^{-1}. This analysis utilized an accessory for the attenuated total reflectance technique with a germanium crystal. The thermoanalytical techniques were detailed through TG/DTG and TG-DSC curve infographics, obtained using the Mettler Toledo TGA/DSC equipment. The system was calibrated according to the manufacturer's specifications. The curves were recorded using an α-Al_2O_3 crucible (70.0 μL) with a sample mass of approximately 5.0 mg, under a heating rate of 20˚C·min^{-1}, dry air atmosphere with a flow rate of 60.0 mL·min^{-1} and a temperature range of 30˚C - 1000˚C.

5. Results and Discussions

5.1. Mid-Infrared Spectroscopy

For the C1 complex, a broad band was observed at 3374 cm^{-1}, indicating the presence of a dipole moment due to hydrogen bonding (O-H) interactions [35] [36]. This suggests the presence of water of hydration in the material, a finding that is corroborated by the thermogram and evidenced in the broad absorption band shown in **Figure 1**. In the absorption region between 3060 - 3018 cm^{-1}, low-intensity overlapping peaks are characteristic of the stretching (ν) of the C-H bonds in sp2 hybridized carbons, which are typical of aromatic groups. The ligand 4,4-dimethyl-2,2-bipyridine contains primary carbons within its structure; this is evidenced by an absorption band at 2920 cm^{-1}, with the corresponding absorption range for aliphatic C-H groups being 2960 - 2850 cm^{-1} [35]. Vibrations attributed to C=C and C=N bonds, which are characteristic of aromatic rings, were identified between 1617 and 1556 cm^{-1} [37]. Lastly, in the range of 1416 - 1446 cm^{-1}, the harmonic bands due to angular deformations of the methyl group ($-CH_3$) can possibly be seen [38].

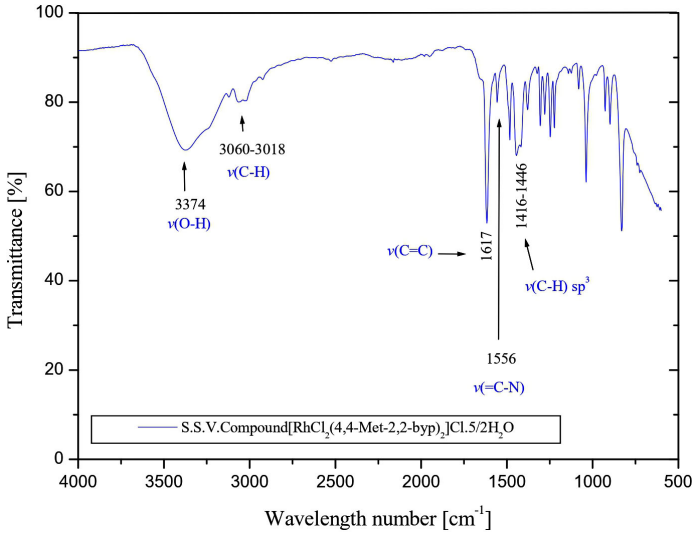

Figure 1. Display of the infrared spectrum and the respective reference peaks.

In a second analysis, the molecular structure of the Isonicotinamide ligand, a primary amide, exhibits two strong bands in the region corresponding to the 3361 cm^{-1} to 3179 cm^{-1} stretches of the ν (N-H) group [30], indicating its presence in this region. However, the compound's hydration water, as observed in the thermogram, leads to an overlap of the peaks corresponding to these stretches. Meanwhile, a band indicative of the carbonyl group ν (C=O) stretching shifts to a lower energy region, presenting an intense peak (**Figure 2**), characteristic of the dipole moment from molecular interactions, at 1683 cm^{-1}, consistent with the L2 ligand peak [35]. The presence of C=C and C=N type vibrations, pertaining to aromatic rings, is evident between 1618 and 1556 cm^{-1} [31] [32]. Additionally, angular deformations linked to the compound's methyl group occur in the range between 1416 and 1446 cm^{-1} [37].

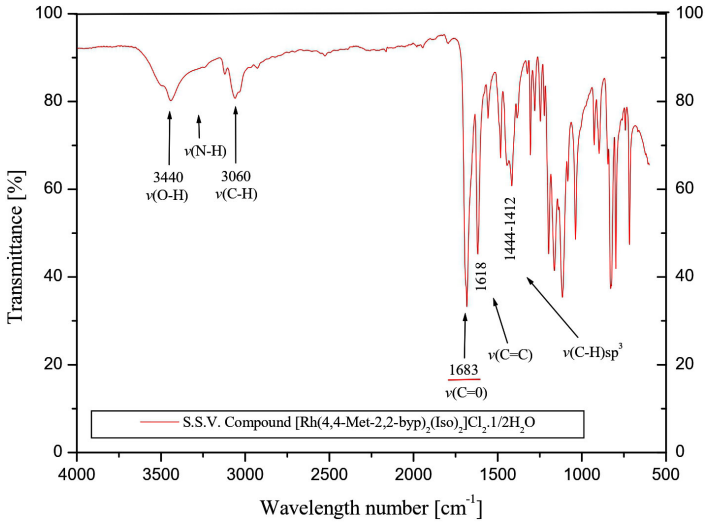

Figure 2. Presentation and comparison of the infrared spectra and the respective reference peaks.

In an attempt to synthesize the third compound, the infrared spectrum was obtained and did not show significant differences between the synthesized compounds, as identified by the vibration bands in Table 1. This observation was consistent both in infrared spectroscopy and in thermogravimetric analysis. The material presented identical behavior to the initial compound (C1), exhibiting the same peaks in their respective analysis regions (Figure 3). Consequently, it is imperative to reexamine the factors that may have interfered with the synthesis, including solubility, temperature, activation energy and chemical stability of the ligand in relation to the metal center, since the reaction did not occur spontaneously as expected.

Table 1. Infrared values obtained for compounds C1, C2, and C3.

	Wave number (CM^{-1})			Vibration band assignment
	C1	C2	C3	
Band intensities found	3376	3500	3377	υ (O-H)
	3240	3120	**	υ (N-H)
	2924	3039 - 2929	3016	υ (C-H)
	*	1683	*	υ (C=O)
	1617 - 1444	1615	1615	υ (C=N); υ (C=C)
	*	1115	1558	δ (N-H)

*No bands; ** Evidence of overlapping bands; U: stretching; δ: angular deformation.

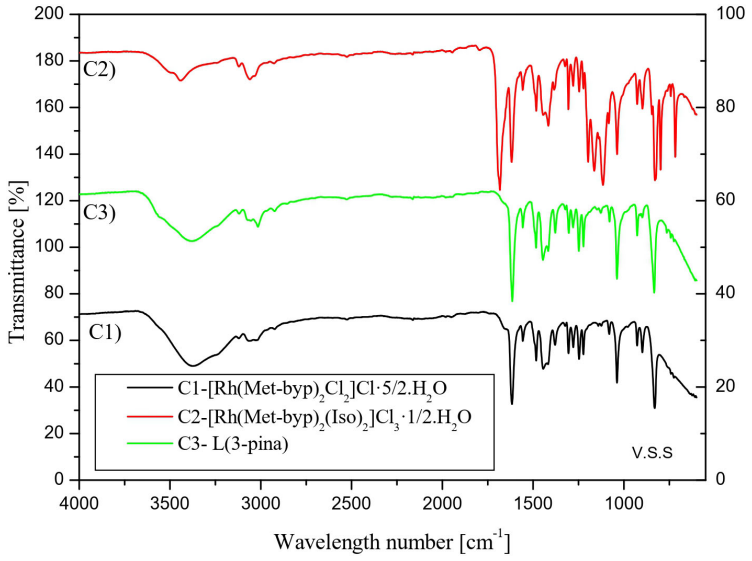

Figure 3. Presentation and comparison of infrared spectra.

5.2. Thermogravimetric Analysis—TG-DTG Curves

The complex $[Rh(Met\text{-}byp)_2Cl_2]Cl{\cdot}5/2H_2O$ demonstrated in this analysis, between 60˚C and 150˚C, a probable loss of hydration water from the synthesized material, as indicated by peaks in the DTG and DSC (Figure 4). This evidence suggests an energy absorption at 100˚C, consisting of an endothermic process [36]. The second thermal event occurred at 300˚C, resulting in a loss of stability and initiating

the decomposition of the material, with a maximum rate of loss observed at 475˚C. During this thermal interval, a single exothermic event was recorded in the DSC (Figure 5), with the maximum peak likely due to sublimation and/or thermal decomposition of the organic compound in the formed complex [39]. Finally, the last stage demonstrated an oxidative event at 503˚C that stabilized at 730˚C, as shown by the TG and DTG curves [40]. This stability was attributed to the presence of an O_2-rich atmosphere, which facilitated the formation of an oxide residue pertaining to the metal in the complex, possibly Rh_2O_3. The significant values in percentages are found in Table 2.

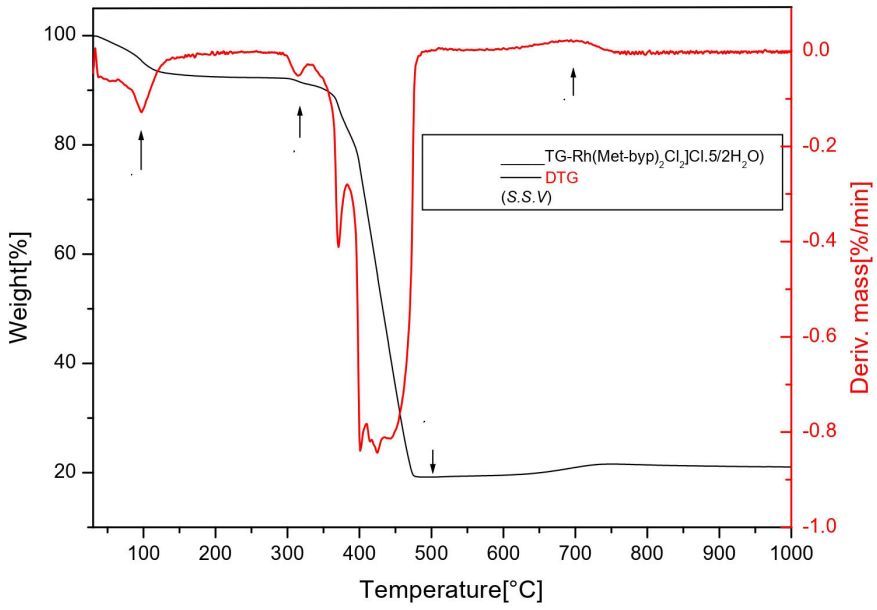

Figure 4. Thermogravimetric curve (TG-DTG) for C1-[Rh(Met-byp)$_2$Cl$_2$]Cl·5/2H$_2$O.

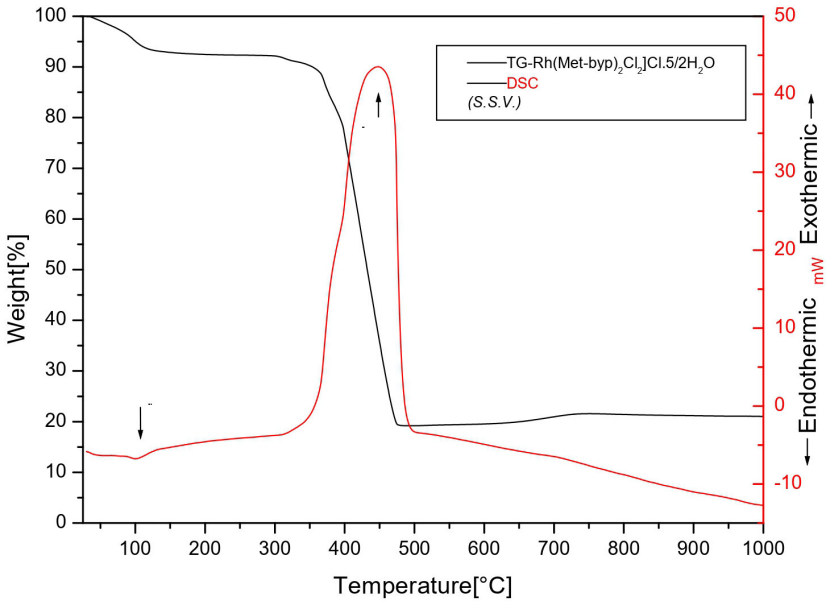

Figure 5. Thermogravimetric curve (TG-DSC) for C1-[Rh(Met-byp)$_2$Cl$_2$]Cl·5/2H$_2$O.

Table 2. Thermogravimetric analysis: percentage values of the TG-DTG curves for the starting compound C1.

Stage	Temperature (˚C)	Loss per % Mass	Error: T-E/T
1	150	7	1.14%
2	300	19	
3	475	73	
4	503	*	

For the modified compound $[Rh(Met\text{-}byp)_2(Iso)_2]Cl_3{\cdot}1/2H_2O$, with the addition of the isonicotinamide ligand, the thermogravimetric curves identified in the TG-DTG are depicted in **Figure 6**, and the thermal behavior as per the DSC is presented in **Figure 7**. During the analysis, it was observed that there were at least three stages of mass loss and one stage of mass gain throughout the thermal analysis process, as indicated in **Table 3**. Initially, between 70˚C - 150˚C, a likely loss of the material's water of hydration was detected, manifesting as a low-intensity peak in both the DTG and DSC, indicative of a possible endothermic process at 100˚C. Subsequent stability was observed up to 173˚C. This stage was succeeded by the second mass loss of the analyte, peaking at 263˚C as evidenced in the DTG, accompanied by the first exothermic reaction of the compound revealed in the DSC. Following this, the material underwent continued thermal decomposition of the organic compounds coordinated to the metal, culminating in a maximal loss at 505˚C. The DSC illustrates a second peak characterized by high energy absorption intensity, thus corroborating the second exothermic reaction of the newly formed compound [36] [41]. In the final stage, a mass gain was recorded, which stabilized at 760˚C [40]. This stabilization is attributed to an O_2-rich atmosphere, thereby facilitating the formation of an oxide under atmospheric conditions and potentially leading to the formation of RhO_2 residue.

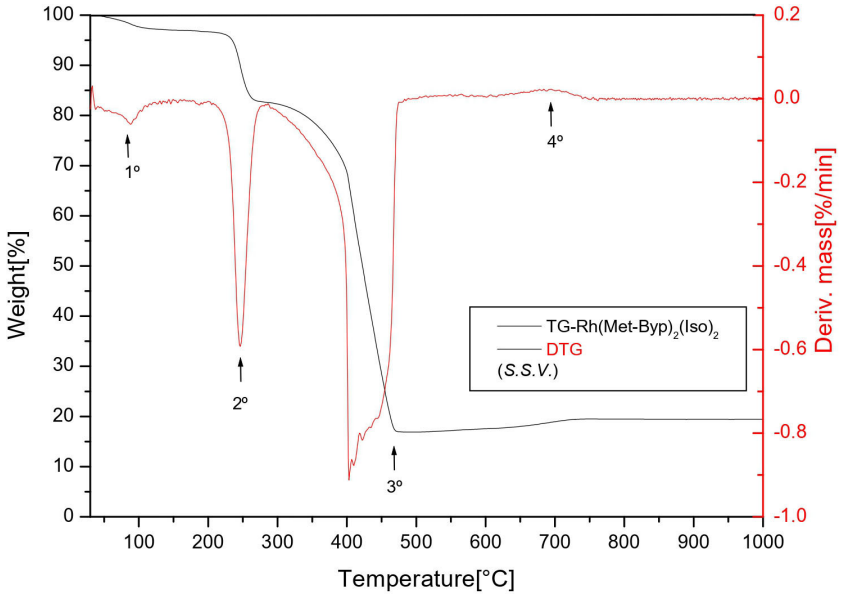

Figure 6. Thermogravimetric curve (TG-DTG) for C2-$[Rh(Met\text{-}byp)_2(Iso)_2]Cl_3{\cdot}1/2H_2O$.

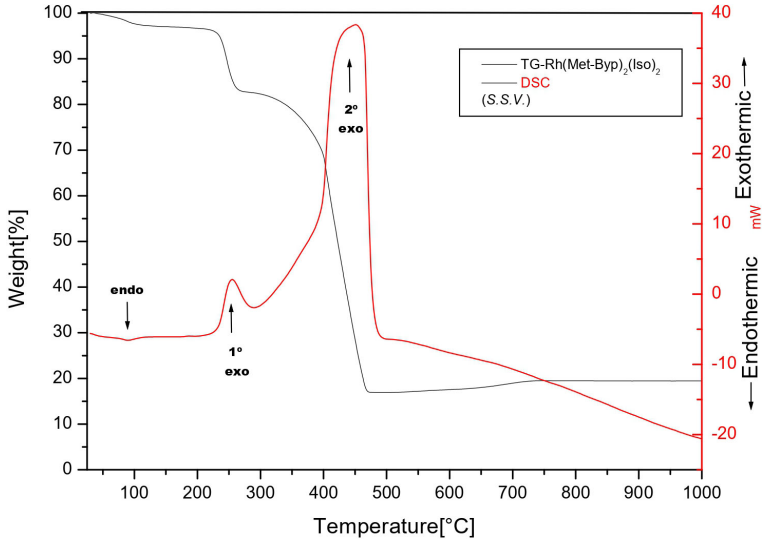

Figure 7. Thermogravimetric curve (TG-DSC) for C2-$[Rh(Met\text{-}byp)_2(Iso)_2]Cl_3{\cdot}1/2H_2O$.

Table 3. Thermogravimetric analysis: percentage values of TG-DTG curves for compound C2.

Stages	Temperature (˚C)	Loss per % Mass	Error: T-E/T
1	160	3	0.44%
2	263	13	
3	505	79	
4	526	*	

*Oxidative event.

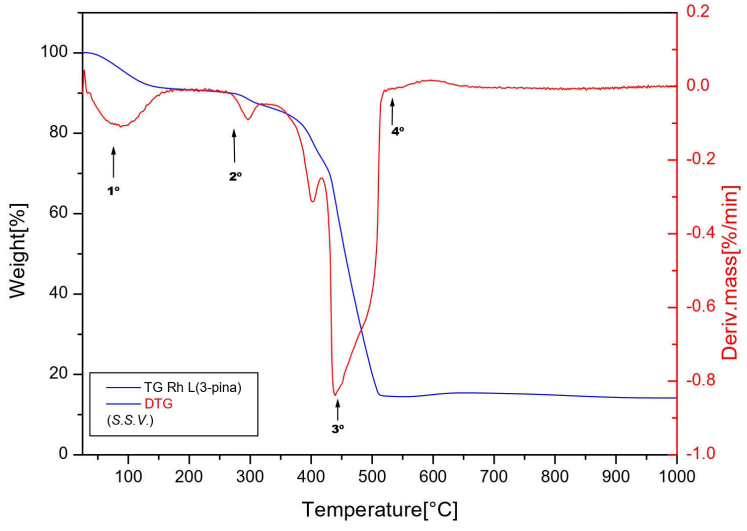

Figure 8. TG-DTG curve of the synthesis compound with L = (3-pina).

For the compound synthesized with the second ligand (3-pina), the following thermogravimetric analyses were conducted: TG-DTG (**Figure 8**) and TG-DSC (**Figure 9**). The initial stage of the analysis identified the loss of volatile compounds

and water of hydration. During the second phase, at 297˚C, the material exhibited the initial stage of thermal decomposition of its coordination sphere. The maximum rate of decomposition was observed at 530˚C. At the conclusion of the analysis, an oxidative stage of the material was identified [40], resulting in an oxide residue that stabilizes at 600˚C. Despite these findings, it was noted that the formation of a new coordinated complex did not occur. This observation was based on the similarities in the consecutive peaks observed in the TG-DTG and the thermal processes in the DSC (**Figure 9**), when compared to the initial synthesis compound depicted in **Figure 4** [41].

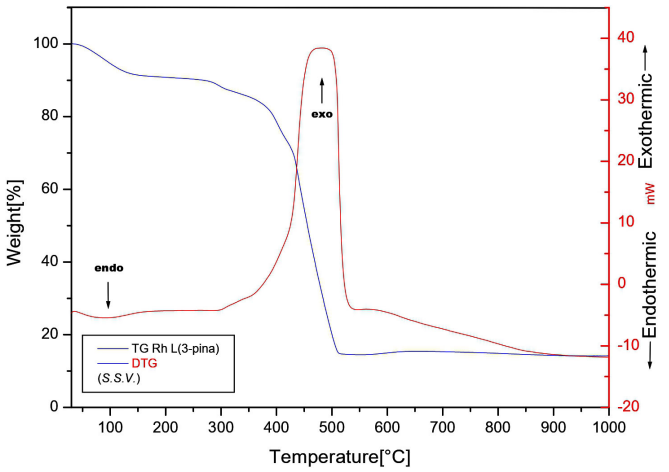

Figure 9. TG-DSC curve of the synthesis compound with L = (3-pina).

6. Cell Viability

Cell viability analysis revealed that after incubation with the compounds, the cells were not adversely affected by compounds C1 and C2 as identified in **Figure 10**. This analysis employed a technique that enabled the quantification of viable cells based on their capacity to absorb light [42] when stained with acridine orange [31]. This stain qualitatively distinguishes live cells, which appear green, from dead cells, which are identified as red or orange. The results indicated that the average viability was in the range of $95 \leq x < 100$, with standard deviations between $3.29 \leq x \leq 4.44$ for live cells, as detailed in **Figure 11** and **Table 4**.

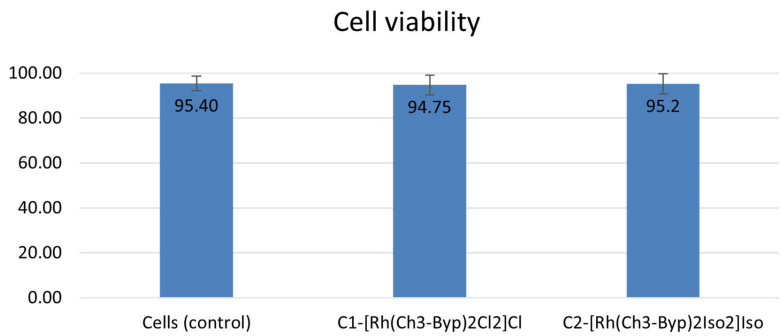

Figure 10. Analysis of cell viability for compounds C1 and C2.

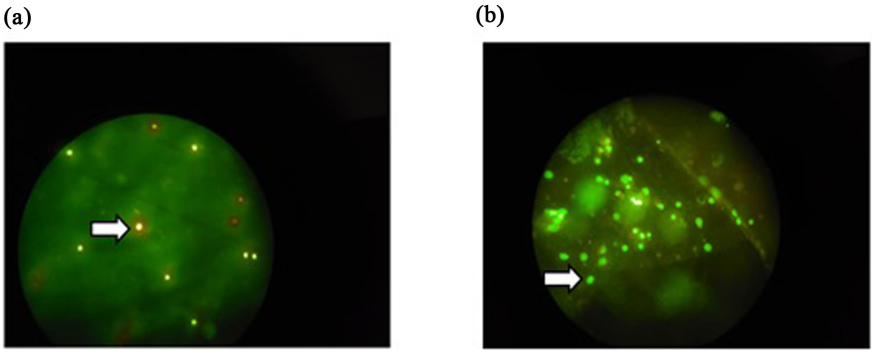

Figure 11. Analysis of peripheral blood mononuclear cells using a fluorescence microscope. (a) Dead cells (red/orange) and (b) Live cells (green).

Table 4. Values in % for cell viability.

Sample groups	Viability (%)	Standard deviation
Cells -(control)	95.40	3.29
C1-[$RhCl_2$(4,4'-Met-2,2'-bipy)$_2$]Cl·5/2H_2O	94.75	4.35*
C2-[Rh(4,4'-Met-2,2'-bipy)$_2$(Iso)$_2$]Cl_3·1/2H_2O	95.2	4.44*

*ANOVA: Statistically significant difference if $p < 0.05$. Data obtained $p = 0.94$.

7. Conclusion

This study proposes two reproducible synthesis routes for two new rhodium(III) ion coordination compounds and suggests the respective minimum stoichiometric formulae: for compound C1-[$RhCl_2$(4,4'-Met-2,2'-bipy)$_2$]Cl·5/2H_2O] and for compound C2-[Rh(4,4'-Met-2,2'-bipy)$_2$(Iso)$_2$]Cl_3·1/2H_2O. These formulae were derived from calculations obtained by thermogravimetric analysis. However, the proposed synthesis for compound C3, involving the nucleophilic substituent (3-pina), revealed that after recrystallization, no evidence of the intended ligand substitution in the starting compound was observed. The inability to identify its coordination using validated analytical techniques indicates a need for further studies to revise the synthesis approach for this new complex. The complex salts, C1 and C2, exhibited solubility in aqueous media and thermal stability as evidenced by thermogravimetric analysis, suggesting their synthesis was successful in coordinating organic ligands to the metal center. Consequently, these compounds were deemed suitable for further testing. In assessments of cell viability, biological tests conducted to evaluate the bioavailability of these complexes revealed that neither compound exhibited cytotoxicity towards human peripheral blood mononuclear cells under specified reference conditions.

Acknowledgements

The authors kindly acknowledge the Federal University of Mato Grosso (UFMT), Materials Research Laboratory (LEMAt), the Maternal and Child Immunology Laboratory (LabImuno), and Coordination for the Improvement of Higher Education Personnel (CAPES).

Authors' Contributions

Conceptualization, Wagner Santos; Data curation, Vanessa Souza; Formal analysis, Vanessa Souza; Research, Aron Carlos, Joyce Laura and Maria José; Methodology, Vanessa Souza; Project management, Wagner Santos; Resources, Adenilda Honório-França, Eduardo França, Joyce Laura and Wagner Santos; Software, Rans Miler, Dayanne Oliveira, Bruna Alves and Sara Cristina; Supervision, Wagner Santos; Validation, Vanessa Souza; Visualization, Vanessa Souza; Writing—original draft, Vanessa Souza; Writing—revision and editing, Wagner Santos.

Conflicts of Interest

The authors declare no conflicts of interest regarding the publication of this paper.

References

[1] Bray, F., Laversanne, M., Sung, H., Ferlay, J., Siegel, R.L., Soerjomataram, I., *et al.* (2024) Global Cancer Statistics 2022: GLOBOCAN Estimates of Incidence and Mortality Worldwide for 36 Cancers in 185 Countries. *CA*: *A Cancer Journal for Clinicians*, **74**, 229-263. https://doi.org/10.3322/caac.21834

[2] Soerjomataram, I. and Bray, F. (2021) Planning for Tomorrow: Global Cancer Incidence and the Role of Prevention 2020-2070. *Nature Reviews Clinical Oncology*, **18**, 663-672. https://doi.org/10.1038/s41571-021-00514-z

[3] Chatelier, E., Mahieu, R., Hamel, J., Chenouard, R., Lozac'h, P., Sallé, A., *et al.* (2020) Pasteurella Bacteraemia: Impact of Comorbidities on Outcome, Based on a Case Series and Literature Review. *International Journal of Infectious Diseases*, **92**, 89-96. https://doi.org/10.1016/j.ijid.2020.01.003

[4] Lai, F.T.T., Liu, W., Hu, Y., Wei, C., Chu, R.Y.K., Lum, D.H., *et al.* (2023) Elevated Risk of Multimorbidity Post-Covid-19 Infection: Protective Effect of Vaccination. *QJM*: *An International Journal of Medicine*, **117**, 125-132. https://doi.org/10.1093/qjmed/hcad236

[5] Ministério da Saúde do Governo Federal Brasil (2022) Instituto de Câncer, Estimativa 2023: Incidência de câncer no Brasil/Instituto Nacional de Câncer. https://ninho.inca.gov.br/jspui/bitstream/123456789/13748/1/Estimativa%202023%20-%20incid%c3%aancia%20de%20c%c3%a2ncer%20no%20Brasil.pdf

[6] Plummer, M., de Martel, C., Vignat, J., Ferlay, J., Bray, F. and Franceschi, S. (2016) Global Burden of Cancers Attributable to Infections in 2012: A Synthetic Analysis. *The Lancet Global Health*, **4**, e609-e616. https://doi.org/10.1016/s2214-109x(16)30143-7

[7] Aguilar, G.R., Swetschinski, L.R., Weaver, N.D., Ikuta, K.S., Mestrovic, T., Gray, A.P., *et al.* (2023) The Burden of Antimicrobial Resistance in the Americas in 2019: A Cross-Country Systematic Analysis. *The Lancet Regional Health—Americas*, **25**, Article ID: 100561. https://doi.org/10.1016/j.lana.2023.100561

[8] Beraldo, H. (2011) Tendências atuais e as perspectivas futuras da química inorgânica. *Ciência e Cultura*, **63**, 29-32. https://doi.org/10.21800/s0009-67252011000100012

[9] Rosenberg, B., Vancamp, L., Trosko, J.E. and Mansour, V.H. (1969) Platinum Compounds: A New Class of Potent Antitumour Agents. *Nature*, **222**, 385-386. https://doi.org/10.1038/222385a0

[10] Weller, M., Tina, O., Rourke, J. and Armstrong, F. (2017) Química Inorgânica. 6th Edition, Bookman.

[11] Souza, M.V.N.D. and Vasconcelos, T.R.A. (2005) Fármacos no combate à tuberculose: passado, presente e futuro. *Química Nova*, **28**, 678-682. https://doi.org/10.1590/s0100-40422005000400022

[12] de Lima, L., Santos, M., Albuquerque, L., Belian, M., Silva, W., Filho, J., *et al.* (2020) Complexos de platina(II) conjugado e análogo a o-glicosídeos: Síntese, caracterização estrutural e atividade antitumoral. *Química Nova*, **43**, 752-759. https://doi.org/10.21577/0100-4042.20170546

[13] Guerra, W., Alves, F.E. and Silva, P.P. (2010) Metais do Grupo da Platina: História, Propriedades e Aplicações. *Boletim da Sociedade Portuguesa de Química*, 27-33. https://doi.org/10.52590/m3.p649.a30001594

[14] Neves, A.P. and Vargas, M.D. (2011) Platinum(II) Complexes in Cancer Therapy. *Revista Virtual de Química*, **3**, 196-209. https://doi.org/10.5935/1984-6835.20110023

[15] dos Santos, E.R. (2011) Síntese e caracterização de complexos de fórmula geral [Ru(AA)(P-P)(N-N)]PF6, onde (AA = aminoácidos; P-P = bifosfinas; N-N = 2, 2'-bipiridina e derivados e 1, 10-fenantrolina): Avaliação de suas potencialidades citotóxicas. https://repositorio.ufscar.br/handle/ufscar/6213

[16] Lima, A.P., Pereira, F.C., Almeida, M.A.P., Mello, F.M.S., Pires, W.C., Pinto, T.M., *et al.* (2014) Cytoxicity and Apoptotic Mechanism of Ruthenium(II) Amino Acid Complexes in Sarcoma-180 Tumor Cells. *PLOS ONE*, **9**, e105865. https://doi.org/10.1371/journal.pone.0105865

[17] Katsaros, N. and Anagnostopoulou, A. (2002) Rhodium and Its Compounds as Potential Agents in Cancer Treatment. *Critical Reviews in Oncology/Hematology*, **42**, 297-308. https://doi.org/10.1016/s1040-8428(01)00222-0

[18] Prathima, T.S., Choudhury, B., Ahmad, M.G., Chanda, K. and Balamurali, M.M. (2023) Recent Developments on Other Platinum Metal Complexes as Target-Specific Anticancer Therapeutics. *Coordination Chemistry Reviews*, **490**, Article ID: 215231. https://doi.org/10.1016/j.ccr.2023.215231

[19] Alessio, E. (2016) Thirty Years of the Drug Candidate NAMI-A and the Myths in the Field of Ruthenium Anticancer Compounds: A Personal Perspective. *European Journal of Inorganic Chemistry*, **2017**, 1549-1560. https://doi.org/10.1002/ejic.201600986

[20] Chaves, J.D.S., Tunes, L.G., de J. Franco, C.H., Francisco, T.M., Corrêa, C.C., Murta, S.M.F., *et al.* (2017) Novel Gold(I) Complexes with 5-Phenyl-1,3,4-Oxadiazole-2-Thione and Phosphine as Potential Anticancer and Antileishmanial Agents. *European Journal of Medicinal Chemistry*, **127**, 727-739. https://doi.org/10.1016/j.ejmech.2016.10.052

[21] de Paiva, R.E.F., Marçal Neto, A., Santos, I.A., Jardim, A.C.G., Corbi, P.P. and Bergamini, F.R.G. (2020) What Is Holding Back the Development of Antiviral Metallodrugs? A Literature Overview and Implications for SARS-CoV-2 Therapeutics and Future Viral Outbreaks. *Dalton Transactions*, **49**, 16004-16033. https://doi.org/10.1039/d0dt02478c

[22] Yu, W., Ping Cheng, L., Pang, W. and Ling Guo, L. (2022) Design, Synthesis and Biological Evaluation of Novel 1, 3, 4-Oxadiazole Derivatives as Potent Neuraminidase Inhibitors. *Bioorganic & Medicinal Chemistry*, **57**, Article ID: 116647. https://doi.org/10.1016/j.bmc.2022.116647

[23] Rocha, D.P., Pinto, G.F., Ruggiero, R., Oliveira, C.A.d., Guerra, W., Fontes, A.P.S., *et al.* (2011) Coordenação de metais a antibióticos como uma estratégia de combate à resistência bacteriana. *Química Nova*, **34**, 111-118.

https://doi.org/10.1590/s0100-40422011000100022

[24] Tulchinsky, Y., Kozuch, S., Saha, P., Mauda, A., Nisnevich, G., Botoshansky, M., *et al.* (2015) Coordination Chemistry of N-heterocyclic Nitrenium-Based Ligands. *Chemistry—A European Journal*, **21**, 7099-7110. https://doi.org/10.1002/chem.201405526

[25] Holmes, J., Pask, C.M. and Willans, C.E. (2016) Chelating N-Heterocyclic Carbene-Carboranes Offer Flexible Ligand Coordination to Ir^{III}, Rh^{III} and Ru^{II}: Effect of Ligand Cyclometallation in Catalytic Transfer Hydrogenation. *Dalton Transactions*, **45**, 15818-15827. https://doi.org/10.1039/c6dt02079h

[26] Gardner, T.S., Wenis, E. and Lee, J. (1954) The Synthesis of Compounds for the Chemotherapy of Tuberculosis. IV. the Amide Function. *The Journal of Organic Chemistry*, **19**, 753-757. https://doi.org/10.1021/jo01370a009

[27] da Encarnação Amorim, K.A. (2020) Sintese, Caracterização e Avaliação Biológica Para Os Compostos De Coordenação De Rutênio(II) E Rutênio(III) Utilizando o Ligante N-(3-Piridil)-Isonicotinamida. Ph.D. Thesis, Universidade Federal de Mato Grosso.

[28] Gerisch, M., Krumper, J.R., Bergman, R.G. and Tilley, T.D. (2002) Rhodium(III) and Rhodium(II) Complexes of Novel Bis(Oxazoline) Pincer Ligands. *Organometallics*, **22**, 47-58. https://doi.org/10.1021/om0207562

[29] dos Santos, W.B., Amorim, K.A.E., Galvão, A.D., Moraes, F.T., Fortaleza, D.B. and Pavanin, L.A. (2019) Photochemical Properties of *trans*-$[Ru(NH_3)_4(bpa)(L)]^{2+}$ (L = py, isn, 4-acpy or 4-pic). *Photochemistry and Photobiology*, **95**, 1306-1310. https://doi.org/10.1111/php.13133

[30] França, E.L., Honorio-França, A.C., Fernandes, R.T.D.S., Marins, C.M.F., Pereira, C.C.D.S. and Varotti, F.D.P. (2015) The Effect of Melatonin Adsorbed to Polyethylene Glycol Microspheres on the Survival of MCF-7 Cells. *Neuroimmunomodulation*, **23**, 27-32. https://doi.org/10.1159/000439277

[31] Tarso, M.F., Dourado, G.A., Batista, F.D., Encarnação, A.K.A.D., Cristina, S.C., Cristina, H.A., *et al.* (2020) Synthesis, Characterization, and Evaluation of Antitumor Potential in MCF-7 Cells of Ruthenium-Derived Compounds. *Advances in Biological Chemistry*, **10**, 86-98. https://doi.org/10.4236/abc.2020.103007

[32] Galvão, A.D., Moraes, F.T.D., Sousa, C.C.D., Sousa, K.M.D.D., Marchi, P.G.F.D., França, A.C.H., *et al.* (2019) Synthesis and Characterization of a New Compound of Cobalt II with Isonicotinamide and Evaluation of the Bactericidal Potential. *Open Journal of Inorganic Chemistry*, **9**, 11-22. https://doi.org/10.4236/ojic.2019.92002

[33] Fornaciari, B., Juvenal, M.S., Martins, W.K., Junqueira, H.C. and Baptista, M.S. (2023) Photodynamic Activity of Acridine Orange in Keratinocytes under Blue Light Irradiation. *Photochem*, **3**, 209-226. https://doi.org/10.3390/photochem3020014

[34] Vray, B., Hoebeke, J., Saint-Guillain, M., Leloup, R. and Strosberg, A.D. (1980) A New Quantitative Fluorimetric Assay for Phagocytosis of Bacteria. *Scandinavian Journal of Immunology*, **11**, 147-153. https://doi.org/10.1111/j.1365-3083.1980.tb00220.x

[35] Fernandes, N.S., Carvalho Filho, M.A.D.S., Mendes, R.A. and Ionashiro, M. (1999) Thermal Decomposition of Some Chemotherapic Substances. *Journal of the Brazilian Chemical Society*, **10**, 459-462. https://doi.org/10.1590/s0103-50531999000600007

[36] Fernandes, R.P., do Nascimento, A.L.C.S., Carvalho, A.C.S., Teixeira, J.A., Ionashiro, M. and Caires, F.J. (2019) Mechanochemical Synthesis, Characterization, and Thermal Behavior of Meloxicam Cocrystals with Salicylic Acid, Fumaric Acid, and Malic Acid. *Journal of Thermal Analysis and Calorimetry*, **138**, 765-777. https://doi.org/10.1007/s10973-019-08118-7

[37] Pavia, D.L., Lampman, G.M., Kriz, G.S. and Vyvyan, J.R. (2010) Tradução da 4 a edição norte-americana. https://www.academia.edu/39590627/Tradu%C3%A7%C3%A3o_da_4_a_edi%C3%A7%C3%A3o_norte_americana

[38] Silverstein, R.M., Webster, F.X. and Kiemle, D.J. (2010) Identificação Espectrométrica de Compostos Orgânicos. LTC.

[39] Fo'ad, T., Hameed, G.S. and Raauf, A.M.R. (2022) Thermal Analysis in the Pre-Formulation of Amorphous Solid Dispersion for Poorly Water-Soluble Drugs. *International Journal of Drug Delivery Technology*, **12**, 1595-1599. https://doi.org/10.25258/ijddt.12.4.19

[40] Ferreira da Cruz, T., Rodrigues de Andrade, G., Rodrigues da Silva, G., Suniga Tozatti, C.S. and Vizolli Favarin, L.R. (2020) Síntese e caracterização de complexos de cobalto(II) com ligantes orgânicos e avaliação antimicrobiana. *UNESUM-Ciencias. Revista Científica Multidisciplinaria*, **3**, 177-190. https://doi.org/10.47230/unesum-ciencias.v3.n1.2019.137

[41] Wesolowski, M. and Leyk, E. (2023) Coupled and Simultaneous Thermal Analysis Techniques in the Study of Pharmaceuticals. *Pharmaceutics*, **15**, Article 1596. https://doi.org/10.3390/pharmaceutics15061596

[42] Aziz, M.A., Krisnadi, S.R., Handono, B. and Setiabudiawan, B. (2023) Pregnant Human Myometrial 1-41 Cell Viability Test on Vitamin D Administration. *Althea Medical Journal*, **10**, 131-135. https://doi.org/10.15850/amj.v10n3.2750